Article

Not peer-reviewed version

Coffee Pulp Gasification for Syngas Obtention and Methane Production Simulation Using Ni Catalysts Supported on Al2O3 and ZrO2 in a Packed Bed Reactor

Carlos Esteban Aristizábal-Alzate *, Ana Belén Dongil , Manuel Romero-Sáez

Posted Date: 5 September 2023

doi: 10.20944/preprints202309.0245.v1

Keywords: carbon dioxide; methanation; power-to-gas; modeling; biomass valorization

Article

Coffee Pulp Gasification for Syngas Obtention and Methane Production Simulation Using Ni Catalysts Supported on Al_2O_3 and ZrO_2 in a Packed Bed Reactor

Carlos Esteban Aristizábal-Alzate [1,*], Ana Belén Dongil [2] and Manuel Romero-Sáez [1]

[1] Grupo Química Básica, Aplicada y Ambiente – Alquimia, Facultad de Ciencias Exactas y Aplicadas, Instituto Tecnológico Metropolitano – ITM, Medellín, Colombia, carlosaristizabal4808@correo.itm.edu.co (C.E.A-A), manuelromero@itm.edu.co (M.R-S)

[2] Instituto de Catálisis y Petroleoquímica, CSIC, Cantoblanco, 28049 Madrid, España; a.dongil@csic.es (A. B-D)

* Correspondence: carlosaristizabal4808@correo.itm.edu.co

Abstract: The methanation of CO_2 is of great interest in power-to-gas systems and contributes to the mitigation of climate change through carbon dioxide capture and the subsequent production of high value-added products. This study investigated CO_2 methanation with three Ni catalysts supported on Al_2O_3 and ZrO_2, which were simulated using a mathematical model of a packed bed reactor designed based on their chemical kinetics reported in the literature. The simulated reactive system was fed with syngas obtained from residual coffee pulp, obtained after solvent phytochemical extraction process, under several gasification conditions. The results reflect a high incidence of catalyst support, preparation method, and syngas composition on CO_2 conversion and CH_4 selectivity. For all the syngas compositions, Ni/ZrO_2 catalysts show the best values for CO_2 conversion and CH_4 selectivity for Ni/Al_2O_3 catalyst.

Keywords: carbon dioxide; methanation; power-to-gas; modeling; biomass valorization

1. Introduction

Nowadays, the methanation of CO_2, also known as the Sabatier reaction, is of great interest in power-to-gas systems since it produces a substitute natural gas (SNG) and enables the valorization of CO_2 [1]. Furthermore, the resulting methane is a combustible gas and does not present many difficulties in its storage [1,2]. As CO_2 is a cause and promoter of climate change, it is highly desirable to develop new processes that capture and/or reuse it [1–3], and thus avoid the use of fossil fuels, since their combustion generates more greenhouse gas (GHG) emissions [4,5]. Additionally, being a fuel that can result from the reuse of CO_2, in principle a zero or low carbon footprint can be established once it has been burned, as well as biofuels [6].

Moreover, synthesis gas (syngas) feeds, the raw material used for CO_2 methanation, can be obtained from the gasification of renewable sources, such us agro-industrial residues and municipal organic waste, among others [7,8]. This study investigates syngas obtained from coffee pulp, which is conventionally used as fertilizer, animal feed, and/or low-quality fuel and, if not properly treated, it may cause environmental damage [9,10]. Therefore, valorizing coffee pulp promotes green chemical synthesis and follows the principles of circular economy. It also contributes to obtaining high added-value products to base the economy and consumption patterns on more sustainable activities [11]. However, to incorporate the biorefinery concept, the coffee pulp considered is a byproduct after a phytochemical extraction process with solvents to take advantage of all its potential to generate high added value products [8].

Moreover, for the formation of methane from CO_2, there must be enough H_2 [3]. Therefore, this study aims to determine the composition of syngas from coffee pulp gasification using steam as

gasifying agent, varying the ratio of steam-biomass ratio (S/B) and operation temperature. Then, it considers simulation of the catalytic conversion of syngas into methane in a packed bed reactor. Matlab© software is used to solve the mathematical model. Nickel-based catalysts are extensively studied for this reaction and because their high performance/cost ratio [5,12–14], being the Ni catalyst supported on alumina the most widely used at industrial scale [1,12,13]. For this reason, in the present work selected catalysts are based on Ni supported in Al_2O_3, and comparing their performance on the process with ZrO_2 as a support, because this oxide shows higher [15]. Based on chemical kinetic models, a commercial Ni/Al_2O_3 and two Ni/ZrO_2 catalysts are compared in terms of CO_2 and H_2 conversion, CH_4 selectivity, and the molar fraction evolution of these chemical species along the catalyst bed. The evaluation of the reaction system with all compounds in a packed bed reactor simulation for CO_2 methanation allows for a more comprehensive understanding of the process, identification of potential interactions and by-products, and reactor design optimization.

1.1. Syngas from biomass as raw material for methanation catalytic process

Gasification is the thermo-chemical conversion of a carbonaceous fuel, and it is characterized by being endothermic process, meaning it requires a heat source [16]. Therefore, it is performed at high temperatures, typically ranging from 500 to 1400 °C, and can take place under atmospheric or elevated pressures, reaching up to 33 bar [17]. Gasifiers traditionally operate within distinct configurations, including fixed-bed, fluidized-bed, and moving-bed systems[18]. This process involves a partial fuel oxidation by using an oxidizing agent, which could be oxygen, air, steam or mixtures of them [19,20]. Despite using air as a gasifying agent is cheap, the syngas dilution by the N_2 presence can lead to a reduction in its high heating value, as well as a decrease in the overall efficiency of the gasification process [21]. Utilizing steam as the gasifying agent leads to the formation of a syngas characterized by its elevated calorific value, typically ranging from 10 to 15 MJ N/m3, and a hydrogen-rich composition [20]. Additionally, [22] highlights the outcomes of syngas generation through biomass gasification with steam. This work demonstrates a yield enhancing of both hydrogen and carbon dioxide, while also presenting a notably higher calorific value in comparison to gasification using oxygen or air as gasifying agents. Therefore, steam is selected as gasifying agent in the present study.

The result of gasification is a fuel gas known as syngas. The main components of syngas are carbon monoxide (CO), hydrogen (H_2), carbon dioxide (CO_2), steam ($H_2O_{(g)}$), methane (CH_4), nitrogen (N_2) if the oxidation agent is air or a mixture of it with other agents, some hydrocarbons in very low quantity and contaminants, such as carbon particles, tar, and ash [16,23]. In the existing literature, the typical syngas composition derived from agro-industrial waste exhibits a hydrogen content falling within the range of 40% to 50%, carbon monoxide at 9.97% to 12.38%, carbon dioxide levels ranging between 25.04% and 26.50%, and consistently maintains methane levels below 0.5%. [24]. However, the final syngas composition depends of operational parameters, the type of biomass and gasifier configuration [23].

Syngas can be used as raw material to heat, generate electricity, or to synthesize high added-value chemical and fuel products through several conversion routes, such as a methanol or synthetic fuels production [8,11]. Therefore, biomass gasification has been considered a viable option for the conversion/utilization of a variety of feedstocks such as vegetable waste, agro-waste, industrial waste, kitchen waste, food waste, and agricultural waste, and even the key to a successful substitution of petroleum derivatives [25,26]. The conditions for this obtention are described in materials and method section.

1.2. Catalytic methane production

In CO_2 methanation, catalysts are needed to achieve high reaction rates, high conversions during CO_2 hydrogenation, and high selectivity towards methane formation [1,14]. The more reported active metal phases used in this reaction are Ni, Ru, Rh, and Co, [1,5,12]. Nickel-based catalysts have been subjected to comprehensive investigation across diverse conditions, owing to their economic advantage and comparatively heightened catalytic activity [5]. In addition, CO_2 methanation

Preprints (www.preprints.org) | NOT PEER-REVIEWED | Posted: 5 September 2023 doi:10.20944/preprints202309.0245.v1

performance is affected by the nature of the catalyst support because it plays an important role in the dispersion of active-metallic sites and metal-support interaction [27], being the more used various metal oxides (e.g., Al_2O_3, TiO_2, SiO_2, ZrO_2, and CeO_2) [5]. Figure 1 is a schematic of the catalytic reaction system that was applied here in a packed bed reactor operating on the gas phase.

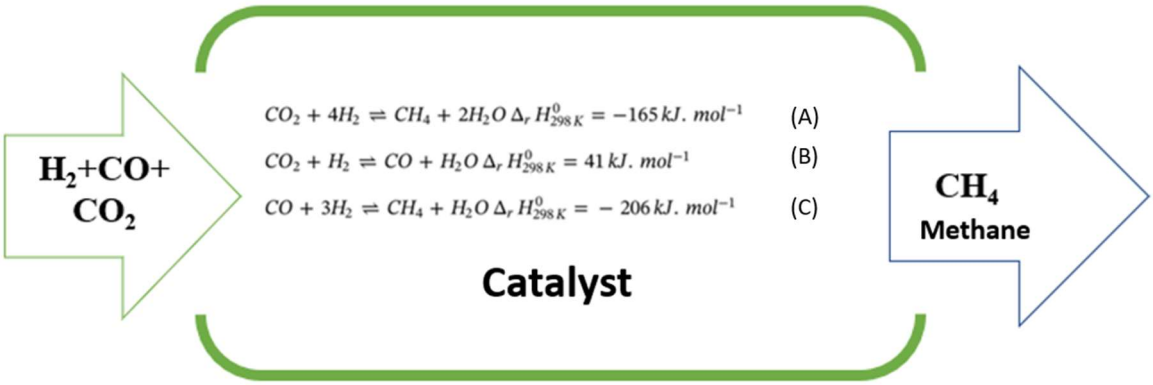

Figure 1. Schematic of the catalytic reaction system for a CO_2 methanation process. Source: Own work.

In Figure 1, (A) indicates the chemical reaction of CO_2 methanation; (B) the Reverse Water Gas Shift (RWGS) reaction; and (C) CO methanation. The carbon dioxide methanation reaction is exothermic and favored at high pressures and low temperatures [1]. The RWS reaction interferes with the selectivity towards methane production. In theory, CO_2 methanation is more favorable an H_2/CO_2 ratio equal to or greater than the stoichiometric ratio (4:1) [14].

The catalysts employed in the methanation process are highly susceptible to the presence of impurities in the stream. These impurities can lead to catalyst poisoning and deactivation, thereby diminishing the catalytic performance and overall efficiency [4,28]. The impurities including chlorine and sulfur compounds, ammonia, tars, and particulate matter [28]. The formation of carbon deposits on nickel-based catalysts during the CO methanation reaction has been extensively investigated, and can be a significant problem, but it does not pose a concern during the CO_2 methanation reaction [4]. Therefore, it is better to use a syngas with higher CO_2 content than CO as a carbon source. Furthermore, the H_2S presence in the syngas should be analyzed if a real operation is considered.

1.3. Ni/ZrO_2 catalyst

In the present work, the kinetic information was taken from [29]. In the latter, the two Ni/ZrO_2 catalysts were tested for methane production by carbon dioxide hydrogenation. Catalysts were prepared using the incipient wetness impregnation method. According to [29], the impregnated sample was calcinated to obtain NiO/ZrO_2-C at 500°C for 3 hours, while NiO/ZrO_2-P was synthesized using dielectric barrier discharge (DBD) plasma for 1 hour. Subsequently, the oxidized metal catalysts were subjected to hydrogen reduction at elevated temperatures to form Ni/ZrO_2-C and Ni/ZrO_2-P.

The chemical kinetics proposed in that study did not include a model such as the Langmuir – Hinshelwood – Hougen –Watson kinetics, which explicitly considers mass transfer in the chemical kinetics. However, simple power-law kinetics for direct reactions can be used for technical applications [30]. Although, CO selectivity for this kinetic does not allow due to it only considers reaction (1). Then, the kinetic model of Ni/ZrO_2 catalysts follows a power-law model, as shown in Equation (1).

$$-r'_{CO2} = \frac{A}{(R\prime * T)^{\propto+\beta}} e^{\frac{-Ea}{R*T}} * P_{CO2}^{\propto} * P_{H2}^{\beta} \quad (1)$$

Where $-r'_{CO}$ is the kinetic rate for CO_2; A, is a pre-exponential factor related with chemical kinetics in (L/g*h); R, the ideal constant of gases ($8.314*10^{-3}$ kJ/mol); R', the ideal constant of gases

Preprints (www.preprints.org) | NOT PEER-REVIEWED | Posted: 5 September 2023 doi:10.20944/preprints202309.0245.v1

(0.082 atm*L/K*mol); Ea, the activation energy in kJ/mol; T, the reaction temperature in K, and P_{CO2}, and P_{H2}, the partial pressure of the CO_2 and H_2 in atm, respectively. Table 1 shows the values of the chemical kinetic model of the two Ni/ZrO_2 catalysts.

Table 1. Kinetic parameters of Ni/ZrO_2 catalysts [29].

Catalyst	E_a (kJ mol^{-1})	α	β	A (L g^{-1} h^{-1})
Ni/ZrO_2-P	93.61	0.65	0.29	2.48×10^{10}
Ni/ZrO_2-C	93.12	0.44	0.54	6.93×10^{9}

1.4. Commercial Ni/Al_2O_3 catalyst

CO_2 methanation reaction with a 14–17 wt.% Ni/Al_2O_3 commercial catalyst is studied in the present work, based on the kinetic model established in [1]. The main rate expressions for CO_2 methanation, CO methanation, and RWGS used in the present study are detailed in Equations (2)–(4), respectively.

$$r'_{CO2met} = \frac{k_{CO2meth} * K_{H2} * K_{CO2} * P_{H2} * P_{CO} * \left(1 - \frac{P_{CH4} * P_{H2O}^2}{P_{H2}^2 * P_{CO2} * K_{eq,CO2me}}\right)}{(1 + K_{CO2} * P_{CO2} + K_{H2} * P_{H2} + K_{H2O} * P_{H2O} + K_{CO} * P_{CO})^2} \quad (2)$$

$$r_{,RWGS} = \frac{k_{RWGS} * K_{CO} * P_{CO2} * \left(1 - \frac{P_{CO} * P_{H2O}}{P_{H2} * P_{CO} * K_{eq,RWGS}}\right)}{(1 + K_{CO2} * P_{CO2} + K_{H2} * P_{H2} + K_{H2O} * P_{H2O} + K_{CO} * P_{CO})} \quad (3)$$

$$r'_{COmeth} = \frac{k_{COme} * K_{H2} * K_{CO} * P_{H2} * P_{CO} * \left(1 - \frac{P_{CH4} * P_{H2O}}{P_{H2}^3 * P_{CO} * K_{eq,COmeth}}\right)}{(1 + K_{CO2} * P_{CO2} + K_{H2} * P_{H2} + K_{H2O} * P_{H2O} + K_{CO} * P_{CO})^2} \quad (4)$$

Where $-r'_i$ is the kinetic rate for each reaction; Ea, the activation energy in kJ/mol; Pi is the partial pressure of component i in bar; Ki is the adsorption constant of component i; Keq,i is the chemical equilibrium constant for reaction i. Table 2 and Table 3 show the adsorption and kinetic parameters, respectively, of this catalyst model.

Table 2. Adsorption parameters of Ni/Al_2O_3 catalyst. [1].

Parameter	K_{CO}	K_{H2O}	K_{CO2}	K_{H2}
Q (KJ/mol)	40.6	14.5	9.72	52.0
Ko (bar^{-1})	$2.39\text{x}10^{-3}$	$6.09\text{x}10^{-1}$	1.07	$5.2\text{x}10^{-5}$

Table 3. Kinetic parameters of Ni/Al_2O_3 catalyst. [1].

Parameter	$k_{CO2,meth}$	k_{RWGS}	$k_{CO,meth}$
Ea (KJ/mol)	110	97.1	97.3
ko (mol/min*g)	$1.14\text{x}10^{8}$	$1.78\text{x}10^{6}$	$2.23\text{x}10^{8}$

2. Results and Discussion

2.1. Syngas description

Preprints (www.preprints.org) | NOT PEER-REVIEWED | Posted: 5 September 2023 doi:10.20944/preprints202309.0245.v1

We performed the gasification of the coffee pulp at two temperatures and two steam/biomass (S/B) ratios. The compositions of the obtained syngas in %V/V are shown in Table 4. S/B ratios were used because steam was the gasifying agent selected in this work. Assuming an ideal gas behavior for syngas, the composition in %V/V is equivalent to molar fraction.

Table 4. Composition of syngas (%V/V) obtained from coffee pulp waste at different temperatures and steam/biomass (S/B) ratios.

Steam/biomass (S/B) ratio	S/B 0.5		S/B 1.0	
Temperature (°C)	700	800	700	800
Hydrogen (%)	48.46	46.51	54.41	50.19
Methane (%)	0.27	0.23	0.25	0.09
Carbon monoxide (%)	24.21	44.06	18.87	37.81
Carbon dioxide (%)	25.05	7.68	24.81	11.39
Ethane (%)	0.14	0.02	0.07	0.03
Ethylene (%)	1.03	0.80	0.59	0.09
Propane (%)	0.74	0.39	0.82	0.37
H_2S (%)	0.1	0.31	0.18	0.03
H_2/CO_2 ratio	1.93	6.06	2.19	4.41

According to the results described in Table 4, the formation of CO_2 is favored under conditions where the S/B ratio is 0.5 and 1.0 at 700 °C. However, there is no significant variation in temperature that allows establishing a better operating condition for this gasification parameter. Although, at a gasification temperature of 700°C, a slightly higher amount of CO_2 is achieved for an S/B ratio of 0.5. On the other hand, higher amounts of H_2 are achieved, like CO_2, for both S/B ratios at 700 °C. Additionally, upon analyzing the considered reactions, CO can contribute to methane formation according to reaction B. Therefore, according to the data in Table 4, better production is achieved for both S/B ratios and temperatures of 800°C. Although, at this temperature, the production of CO_2 is not high as at 700°C. H_2/CO_2 ratios are greater than stochiometric ratio for reaction 1 (4:1), when gasification temperature of 800°C for both S/B ratios is implemented. Furthermore, with S/B of 0.5 better value for this relation is achieved.

According to [20] and [26], as raising the gasification temperature leads to a reduction of chemical species that can poison and enhance catalyst deactivation. However, it is true for the own gasification results when a S/B of 1.0 is used, because in an S/B ratio of 0.5, the behavior is contrary to what is established by these references. Therefore, The S/B ratio could affect the formation of H_2S since there is a clear variation in the formation of this poison agent when comparing both gasification temperatures. To obtain synthesis gases from coffee pulp with the most adequate composition to avoid the possible acceleration of catalyst poisoning and deactivation, the temperature of 800 °C and S/B of 1.0 should be selected, due to it presents the lowest value for H_2S formation in the syngas.

2.2. Catalytic simulation of methanation

Once obtained the syngas compositions after gasification, we analyzed the CO_2 conversion rate, CH_4 selectivity and H_2 conversion throughout the weight catalytic bed (w) of each one of the syngas compositions and catalysts considering the kinetics described above. The results are shown in Figures 2-4.

Preprints (www.preprints.org) | NOT PEER-REVIEWED | Posted: 5 September 2023 doi:10.20944/preprints202309.0245.v1

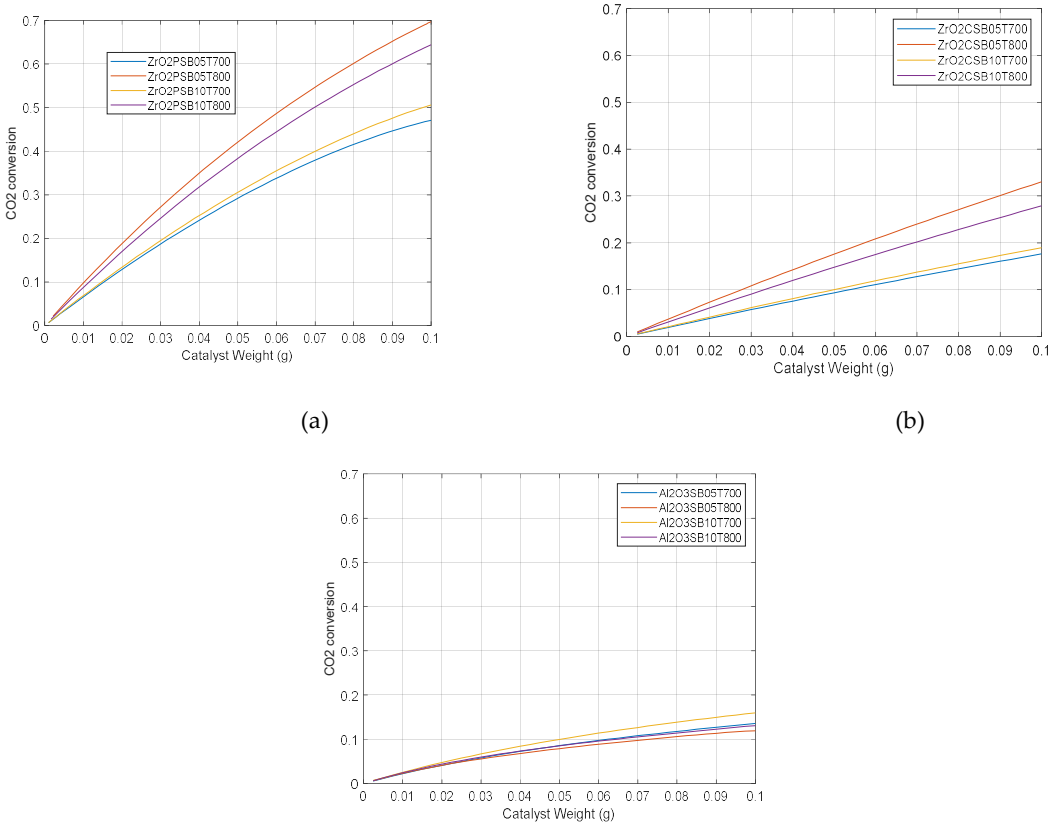

(a) (b)

(c)

Figure 2. CO_2 conversion Ni based catalysts for all syngas composition: (a) Ni/ZrO_2-P, (b) Ni/ZrO_2-C and (c) Commercial Al_2O_3.

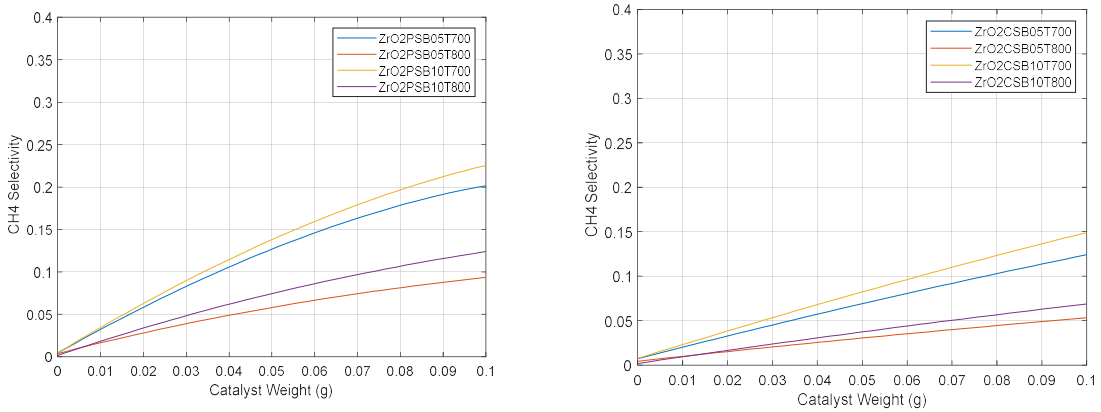

(a) (b)

Preprints (www.preprints.org) | NOT PEER-REVIEWED | Posted: 5 September 2023 doi:10.20944/preprints202309.0245.v1

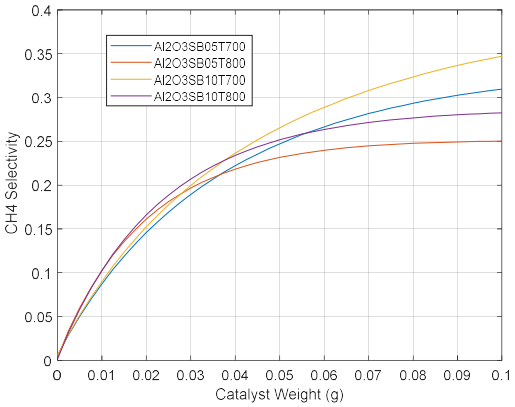

(c)

Figure 3. CH_4 selectivity for Ni based catalysts for all syngas composition: (a) Ni/ZrO_2-P, (b) Ni/ZrO_2-C and (c) Commercial Al_2O_3.

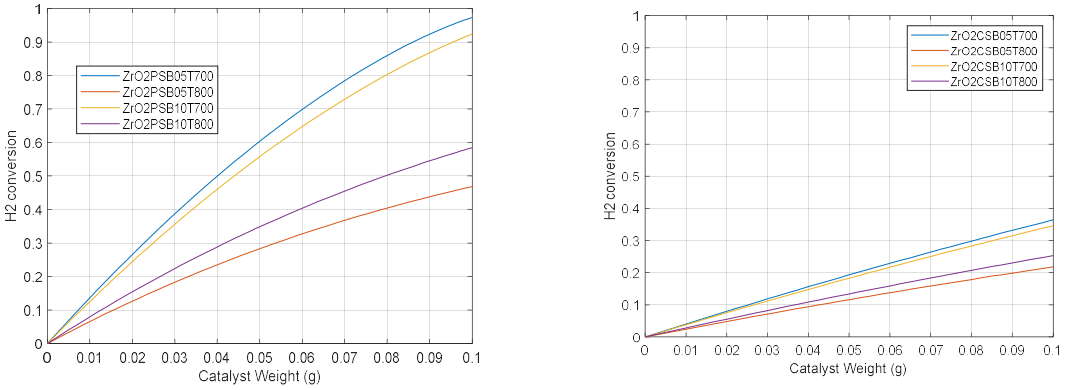

(a) (b)

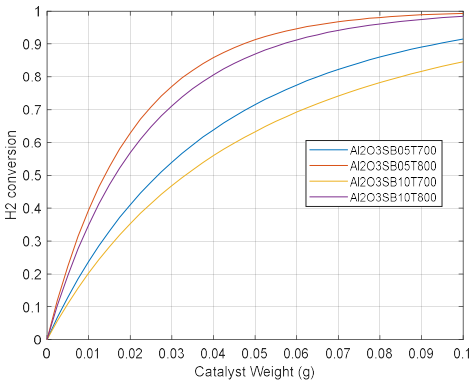

(c)

Figure 4. H_2 conversion Ni based catalysts for all syngas composition: (a) Ni/ZrO_2-P, (b) Ni/ZrO_2-C and (c) Commercial Al_2O_3.

At 800 °C of gasification for both S/B ratios, the feed syngas streams contain a lower concentration of CO_2, resulting in a decreased reactant-to-catalyst ratio, in other words, it has a lower space velocity. This condition leads to higher conversion rates for these gasification process

Preprints (www.preprints.org) | NOT PEER-REVIEWED | Posted: 5 September 2023 doi:10.20944/preprints202309.0245.v1

parameters. To obtain an accurate comparison, it is necessary to evaluate the results obtained at 700 °C and those obtained at 800 °C, separately for all simulated catalysts. In Figure 2, Figure 3 and Figure 4, Ni/ZrO_2-P obtained better results than Ni/ZrO_2-C in terms of CO_2 conversion, H_2 conversion and CH_4 selectivity. In accordance with [29], this behavior is due to a greater number of active sites, which can be provided by highly dispersed Ni particles on Ni/ZrO_2-P, leading to a higher reaction rate for CO_2 methanation. The surface Ni concentration of Ni/ZrO_2-P, estimated at Ni/Zr = 0.18, is higher than Ni/ZrO_2-C catalyst (Ni/Zr = 0.13). Therefore, this indicates a better Ni dispersion on the support induced by plasma decomposition. In addition, it has been proposed that this method of preparation facilitates the partial reduction of ZrO_2 to create more oxygen vacancies, this improving CO_2 activation [29]. For these ZrO_2 supported catalysts, at 700°C is better to use S/B ratio of 1.0 to obtain high conversions for CO_2 and CH_4 selectivity. However, for same temperature, the H_2 conversion is best when Ni/ZrO_2-C catalyst uses a syngas from S/B of 1.0 and for Ni/ZrO_2-P, S/B of 0.5. The highest CH_4 selectivity and H_2 conversion were produced for 800 °C with S/B ratio of 1.0 and CO_2 conversion at S/B of 0.5.

Regarding the results of the commercial Ni/Al_2O_3 catalyst in Figure 1 (c) and Figure 2 (c), it achieved the highest values of CO_2 conversion and CH_4 selectivity with a syngas obtained using an S/B ratio of 1.0 for both temperatures in the gasification process. According to Figure 4 (c), the H_2 conversion behavior of this support is opposite to that of the two other parameters for the mentioned S/B gasification condition.

Figure 5 shows the quantitative percentage comparisons of catalysts and their improvement for CO_2 conversion (a), CH_4 selectivity (b) and H_2 conversion (c) at the reactor outlet, using all the syngas compositions. The results are expressed in percentages (%).

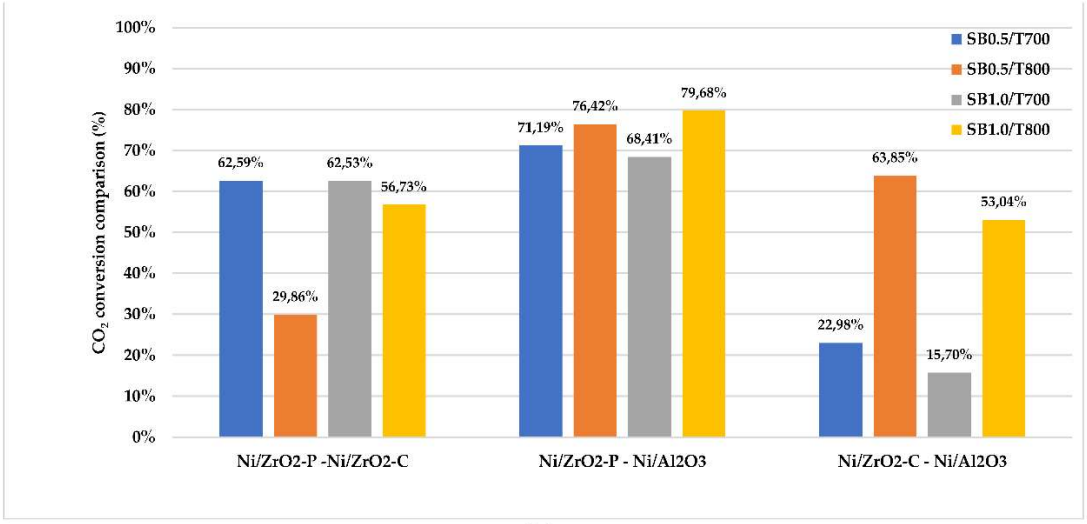

(a)

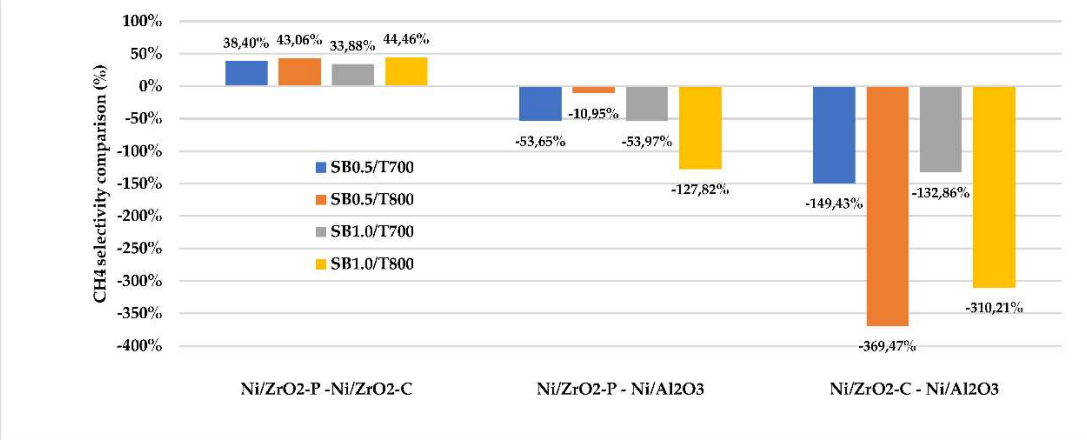

(b)

Preprints (www.preprints.org) | NOT PEER-REVIEWED | Posted: 5 September 2023 doi:10.20944/preprints202309.0245.v1

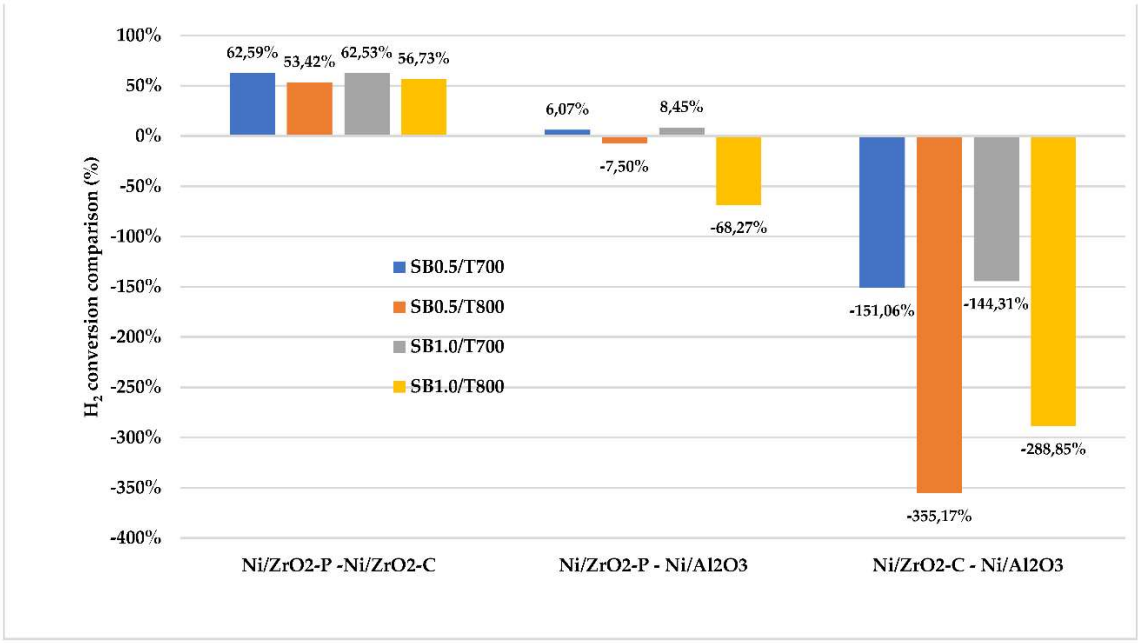

(c)

Figure 5. Comparison in percentage (%) of CO_2 conversion (a), CH_4 selectivity (b) and H_2 conversion (c) of the catalysts under study.

By comparing the catalysts, it is possible to observe in Figure 5, with respect to CO_2 conversion and CH_4 selectivity, the highest values were achieved with ZrO_2 and Al_2O_3 supported catalysts, respectively. This trend is constant for all the syngas compositions examined in this study. This result is in accordance with [15], which reports that the catalytic system exhibited a higher activity with ZrO_2 supports than with their Al_2O_3 counterparts. The CH_4 selectivity produced with Al_2O_3 corroborates what was reported in [27], that this support presents superior methane selectivity. For H_2 conversion, it is better Al_2O_3 support than ZrO_2 supports. However, when synthesis gases from 700°C and both S/B ratios are used with Ni/ZrO_2p catalyst, the H_2 conversions are better than the obtained for Ni/Al_2O_3 commercial catalyst. Additionally, ZrO_2p shows better conversions and selectivity than ZrO_2c. Therefore, the loss of CH_4 selectivity of ZrO_2 catalysts are more significant for the calcination preparation than for the plasma preparation, when compared to the commercial Ni catalyst supported on Al_2O_3.

Since the power-law kinetic model for Ni/ZrO_2 catalysts only include Reaction (A) for CO_2 methanation, it is not possible to stablish the CO selectivity. However, chemical kinetic model for commercial Ni/Al_2O_3 catalyst consider all reactions. Therefore, this catalyst allows to calculate the selectivity for CO, to determine the performance of gasification conditions in Sabatier process to increase CH_4 yield and to minimize the by-products generation. Figure 6 illustrates the CH_4, CO and H_2O selectivity for commercial Ni/Al_2O_3 catalyst considering all the gasification conditions.

Preprints (www.preprints.org) | NOT PEER-REVIEWED | Posted: 5 September 2023 doi:10.20944/preprints202309.0245.v1

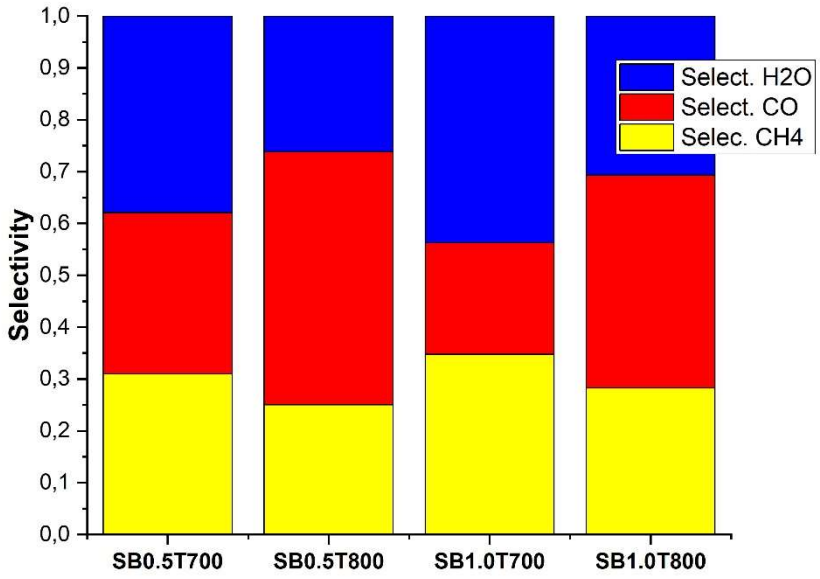

Figure 6. CH_4, CO and H_2O selectivity comparison for commercial Ni/Al_2O_3 catalyst considering all the gasification conditions.

Figure 6 shows a better behavior over Ni/Al_2O_3 catalyst for CO selectivity at 800 °C when S/B of 0.5 is applied. At 700 °C the same effect is shown for S/B of 1.0. Furthermore, with these gasifying conditions CH_4 selectivity are lower. This can be explained by the fact that with these S/B conditions for gasification at the respective temperatures, they have a higher amount of CO and a lower amount of CO_2 in their composition. The selectivity towards H_2O is more marked when S/B is 1.0 for both gasification temperatures. It can be explained because with an S/B ratio at this value, a higher amount of steam is feed.

3. Materials and Methods

This section starts with a detailed description of the biomass gasification procedure for syngas production from coffee pulp after a solvent phytochemical extraction to obtain chlorogenic acid. Then, a theorical kinetic study is considered for methane production using Ni based catalysts on ZrO_2 and Al_2O_3 supports on a packed bed reactor. It presents a mathematical model that includes the assumptions and all the equations that are necessary to simulate a packed bed reactor considering a heterogenous catalyst for the reactive system. Finally, it details the CO_2 conversion, H_2 conversion and CH_4 selectivity of the model constructed here when it was simulated with each catalyst, using its respective chemical kinetic parameters found in the cited references.

3.1. Gasification experimental system

These residual coffee pulps are taken as a solid filtered after a solvent phytochemical extraction process using ethanol/H_2O (70/30 %V/V) at ambient temperature, atmospheric pressure and coffee pulp-to-solvent ratio of 1 to 4. They were subjected to gasification using a horizontal furnace reactor. The reactor comprises a quartz tube with an external diameter of 3.5 cm (internal diameter of 3.0 cm) and a length of 50 cm. The quartz tube is inserted into the annular space of the 40 cm long horizontal furnace. The furnace is heated by electric resistances and its temperature is controlled through a proportional-integral-derivative (PID) loop, enabling continuous monitoring of the reactor temperature. To facilitate the gasification process, the sample was loaded into a 2.0 cm diameter and

Preprints (www.preprints.org) | NOT PEER-REVIEWED | Posted: 5 September 2023 doi:10.20944/preprints202309.0245.v1

13.5 cm length quartz sample holder within the reactor. Inside the sample holder, a K-type thermocouple was inserted to accurately measure the temperature of the sample bed.

The gasification experiments were conducted at two different temperatures: 700 °C and 800 °C. Additionally, two steam-to-biomass ratios (S/B) were tested, namely 0.5 and 1.0, to evaluate their effects on the gasification process.

The produced syngas was analyzed using an Agilent Micro GC model 3000. This analytical instrument is equipped with two thermal conductivity detectors (TCD). One TCD utilizes a 10 m x 0.32 mm 5A molecular sieve column with argon as the carrier gas, while the other TCD employs an 8 m x 0.32 mm column with helium as the carrier gas.

3.2. Mathematical model for the methanation catalytic packed bed reactor simulation

This subsection discusses the simulation of a packed bed reactor operating in steady-state conditions. The conditions of the reactor were a total inlet molar flux of 0.1 mol/min, ambient pressure, and 400 °C as in [26]. Although this temperature does not achieve the highest conversion of CO_2, it offers the best CH_4 selectivity. In the simulation, the reactor considers a catalyst weight of 100 mg in a packed bed configuration at 1 atm. These conditions were maintained constant in all the simulations to be able to compare the behavior of the catalysts using the syngas compositions described above. The following considerations and simplifications proposed by [31] and [32] were implemented for this type of operation and reactor:

- Negligible radial diffusion: concentration and temperature profiles are assumed to be constants, which leads to a one-dimensional model.
- Constant radial speed.
- Temperature and pressure profiles in the catalyst are assumed to be constants (homogeneous catalytic particle).
- As in [13], the mechanisms related to catalyst deactivation, such as sulfur poisoning or carbon formation via the Boudouard reaction, are not taken into consideration or disregarded in the present study.

As the process is carried out in a packed bed reactor, the resulting model must be adjusted to the design equation of this type of reactor, which can be consulted in [13]. Equations (4)–(8) are the system of ordinary differential equations (ODEs) used here for the mass balance and reactor design. They express each reactive species involved in the Sabatier process.

$$\frac{dF_{CO}}{dW} = r'_{CO} \tag{4}$$

$$\frac{dF_{CO2}}{dW} = r'_{CO} \tag{5}$$

$$\frac{dF_{H2}}{dW} = r'_{H2} \tag{6}$$

$$\frac{dF_{CH4}}{dW} = r'_{CH4} \tag{7}$$

Preprints (www.preprints.org) | NOT PEER-REVIEWED | Posted: 5 September 2023 doi:10.20944/preprints202309.0245.v1

$$\frac{dF_{H2O}}{dW} = r'_{H2O} \tag{8}$$

Where Fi denotes the molar flux of species i; r'i, the chemical kinetics of species i; and W, the catalyst weight inside the heterogeneous reactor in grams.

Since the system has three chemical reactions in parallel: (1) CO_2 methanation, (2) RWGS, and (3) CO methanation, it should consider the species that appear in more than one of these reactions because the chemical kinetics of each of said reactions are coupled and given in parallel as well. Equations (16)–(20) show the global or total reactions for each species involved in the process described above, where each r_i is expressed in mol/min.g_{cat}.

$$r'_{CO2} = -(r'_{CO2-met} + r'_{RWGS}) \tag{16}$$

$$r'_{H2} = -(4.r'_{CO2-met} + r'_{RWGS} + 3.'r_{CO-met}) \tag{17}$$

$$r'_{CH4} = r'_{CO2-met} + r'_{CO-met} \tag{18}$$

$$r'_{H2O} = 2.r'_{CO2-met} + r'_{RWGS} + r'_{CO-met} \tag{19}$$

$$r'_{CO} = r'_{RWGS} - r'_{CO-met} \tag{20}$$

Catalyst performance is analyzed here by measuring CO_2 conversion and the selectivity of CH_4, CO and H_2O production. CO_2 conversion and the selectivity of CO_2 to CH_4 and by-products are described in Equation (21) and Equation (22).

$$X_{CO2} = \frac{F_{CO2_{in}} - F_{CO2_{out}}}{F_{CO\ in}} \tag{21}$$

$$S_{CO2/CH4} = \frac{F_{CH4_{out}}}{F_{CO_{out}} + F_{CH\ out} + F_{H2O_{out}}} \tag{22}$$

$$S_{CO2/CO} = \frac{F_{CO_{out}}}{F_{CO_{out}} + F_{CH\ out} + F_{H2O_{out}}} \tag{23}$$

$$S_{CO2/H2O} = \frac{F_{H2O_{out}}}{F_{CO_{out}} + F_{CH\ out} + F_{H2O_{out}}} \tag{24}$$

Where X_{CO2} is the CO_2 conversion inside the reactor and $S_{CO2/CH4}$, $S_{CO2/CO}$ and $S_{CO2/H2O}$ are the selectivity of CO_2 to transform it into CH_4, CO and H_2O, respectively. F_{i_in} and F_{i_out} are the molar flux of components according to the subindex in mol/min.

Most kinetic expressions studied and analyzed here depend on the partial pressures of the chemical species involved, and, since the system of differential equations is based on molar balance. Therefore, Equation (25) must be used to relate the partial pressures to the molar fluxes of each species.

 doi:10.20944/preprints202309.0245.v1

$$P_i = \frac{F_i}{\sum_{i=1}^{n} F_i} * P_T \quad (25)$$

Where P_i is the partial pressure of species i inside the reactor; F_i, the molar flux of component i (mol/min); $\sum_{i=1}^{n} F_i$, the summation of all molar fluxes of the species involved (mol/min); and P_T, the total system pressure.

4. Conclusions

This paper presented a coffee pulp gasification after phytochemical extraction process, varying S/B ratios (0.5 and 1.0) and temperatures (700°C and 800 °C). The resulting syngas is considered as raw material from methane production through Sabatier process. The adequate syngas according to H_2/CO_2 ratio is achieved with 800°C and both S/B ratios because these conditions exceed the stoichiometric ratio (4:1) for the CO_2 methanation reaction. Additionally, the temperature of 800°C reduces the formation of H_2S, what favors to avoid the acceleration of catalyst poisoning. However, in the present study is not considered in the catalyst simulation this effect.

Then, a comparative analysis of three Ni catalysts in terms of CO_2 methanation performance and behavior is considered. Such analysis was based on a mathematical model that simulated their chemical kinetics reported in their respective references, using MATLAB©. The chemical kinetics of the two simulated Ni/ZrO_2 catalysts were taken from [29], where they were prepared adopting two different methods: one was obtained using dielectric barrier discharge (DBD) plasma; and the other, by calcination. In turn, the kinetics of the Ni/Al_2O_3 commercial catalyst, were taken from [1]. This study established CO_2 conversion, CH_4 selectivity and H_2 conversion in CO_2 methanation depending on catalyst preparation method, catalyst support, raw material composition, and gasification process conditions.

According to the results, Ni/ZrO_2-P has a better catalytic behavior than Ni/ZrO_2-C, which corroborates that the catalyst preparation method influences catalyst activity. Also, the catalyst support affects CO_2 conversion, H_2 conversion and CH_4 selectivity. ZrO_2-supported catalysts show better CO_2 conversion, but the Ni/Al_2O_3 commercial catalyst has higher CH_4 selectivity and H_2 conversion. Although, Ni/ZrO_2p catalyst presents better H_2 consumption than commercial Ni/Al_2O_3 for 700°C and both S/B ratios.

Regarding the syngas composition, Ni/Al_2O_3 was more active for CO_2 conversion and selective for CH_4 when an S/B ratio of 1.0 for both temperatures was employed. In contrast, the H_2 conversion is better for S/B of 0.5. Furthermore, ZrO_2-c catalysts had better CO_2 conversion, H_2 conversion and CH_4 selectivity at 700°C using S/B ratio of 1.0 and for 800°C, it favors the CO_2 conversion with S/B of 0.5 and CH_4 selectivity and H_2 conversion at S/B ratio of 1.0. ZrO_2-p the gasification S/B of 1.0 present the best CO_2 conversion and CH_4 selectivity values for 700°C. For 800°C, a S/B of 1.0 improves CH_4 selectivity and H_2 conversion and S/B of 0.5 the CO_2 conversion.

Finally, the model presented in this study has the potential to be applied to evaluate the CO_2 methanation process using different types of syngas derived from various biomass sources and operating conditions during the gasification process. By utilizing the same catalysts studied in this paper, researchers can conduct theoretical exploratory research to quickly estimate the impact of different variables on CO_2 conversion, H_2 conversion and CH_4 selectivity. This approach offers the advantage of saving both time and resources by providing a valuable method to identify the variables at the gasification process that promote favorable CO_2 conversion, CH_4 selectivity and H_2 conversion.

Author Contributions: C.E.A.A conducted the experiments and simulation calculus. Additionally, he wrote the article; C.E.A.A analyzed the data and discussed with A.B.D and M.R.S; A.B.D and M.R.S provided supervision and valuable critical feedback and played a crucial role in finalizing the article. It is important to note that all authors made substantial contributions to the manuscript, collectively enriching its content. All authors have read and agreed to the published version of the manuscript.

Funding: This research received no external funding

Institutional Review Board Statement: The study did not require ethical approval.

Informed Consent Statement: Not applicable.

Data Availability Statement: The data are available upon request.

Conflicts of Interest: The authors declare no conflict of interest

References

1. Champon, A. Bengaouer, A. Chaise, S. Thomas, and A. C. Roger, "Carbon dioxide methanation kinetic model on a commercial Ni/Al2O3 catalyst," J. CO2 Util., vol. 34, no. March, pp. 256–265, 2019, doi: 10.1016/j.jcou.2019.05.030.
2. V. Scharl, F. Fischer, S. Herrmann, S. Fendt, and H. Spliethoff, "Applying Reaction Kinetics to Pseudohomogeneous Methanation Modeling in Fixed-Bed Reactors," Chem. Eng. Technol., vol. 43, no. 6, pp. 1224–1233, 2020, doi: 10.1002/ceat.201900535.
3. K. P. Brooks, J. Hu, H. Zhu, and R. J. Kee, "Methanation of carbon dioxide by hydrogen reduction using the Sabatier process in microchannel reactors," Chem. Eng. Sci., vol. 62, no. 4, pp. 1161–1170, 2007, doi: 10.1016/j.ces.2006.11.020.
4. L. Shen, J. Xu, M. Zhu, and Y. F. Han, "Essential role of the support for nickel-based CO2 methanation catalysts," ACS Catal., vol. 10, no. 24, pp. 14581–14591, 2020, doi: 10.1021/acscatal.0c03471.
5. M. Romero-Sáez, A. B. Dongil, N. Benito, R. Espinoza-González, N. Escalona, and F. Gracia, "CO2 methanation over nickel-ZrO2 catalyst supported on carbon nanotubes: A comparison between two impregnation strategies," Appl. Catal. B Environ., vol. 237, no. March, pp. 817–825, 2018, doi: 10.1016/j.apcatb.2018.06.045.
6. M. Marchi, E. Neri, F. M. Pulselli, and S. Bastianoni, "CO2 recovery from wine production: Possible implications on the carbon balance at territorial level," J. CO2 Util., vol. 28, no. October, pp. 137–144, 2018, doi: 10.1016/j.jcou.2018.09.021.
7. J. H. Clark, "Green chemistry for the second generation biorefinery – sustainable chemica manufacturing based on biomass," J. Chem. Technol. Biotechnol., vol. 82, no. May, pp. 603–609, 2007, doi: 10.1002/jctb.
8. C. E. Aristizábal-Alzate, P. N. Alvarado, and A. F. Vargas, "Biorefinery concept applied to phytochemical extraction and bio-syngas production using agro-industrial waste biomass: A review," Ing. e Investig., vol. 40, no. 2, pp. 22–36, 2020, doi: 10.15446/ing.investig.v40n2.82539.
9. P. Esquivel and V. M. Jiménez, "Functional properties of coffee and coffee by-products," Food Res. Int., vol. 46, no. 2, pp. 488–495, 2012, doi: 10.1016/j.foodres.2011.05.028.
10. P. S. Murthy and M. Madhava Naidu, "Sustainable management of coffee industry by-products and value addition—A review," Resour. Conserv. Recycl., vol. 66, pp. 45–58, 2012, doi: 10.1016/j.resconrec.2012.06.005.
11. C. E. Aristizábal-Alzate, P. N. Alvarado-Torres, and A. F. Vargas-Ramírez, "Simulation of methanol production from residual biomasses in a Cu/ZnO/Al2O3 packed bed reactor," Rev. Fac. Ing., no. 102, pp. 115–124, 2022, doi: 10.17533/udea.redin.20200907.
12. P. A. U. Aldana et al., "Catalytic CO2 valorization into CH4 on Ni-based ceria-zirconia. Reaction mechanism by operando IR spectroscopy," Catal. Today, vol. 215, pp. 201–207, 2013, doi: 10.1016/j.cattod.2013.02.019.
13. S. Rönsch, J. Köchermann, J. Schneider, and S. Matthischke, "Global Reaction Kinetics of CO and CO2 Methanation for Dynamic Process Modeling," Chem. Eng. Technol., vol. 39, no. 2, pp. 208–218, 2016, doi: 10.1002/ceat.201500327.
14. N. D. M. Ridzuan, M. S. Shaharun, M. A. Anawar, and I. Ud-Din, "Ni-Based Catalyst for Carbon Dioxide Methanation: A Review," Catalysts, vol. 12, p. 469, 2022.
15. V. Tongnan et al., "Process intensification of methane production via catalytic hydrogenation in the presence of ni-ceo2/cr2o3 using a micro-channel reactor," Catalysts, vol. 11, no. 10, 2021, doi: 10.3390/catal11101224.
16. Molino, S. Chianese, and D. Musmarra, "Biomass gasification technology: The state of the art overview," J. Energy Chem., vol. 25, pp. 10–25, 2016, doi: 10.1016/j.jechem.2015.11.005.
17. Ahmad, N. A. Zawawi, F. H. Kasim, A. Inayat, and A. Khasri, "Assessing the gasification performance of biomass: A review on biomass gasification process conditions, optimization and economic evaluation," Renew. Sustain. Energy Rev., vol. 53, pp. 1333–1347, 2016, doi: 10.1016/j.rser.2015.09.030.
18. V Bridgwater, "The technical and economic feasibility of biomass gasification for power generation," vol. 14, no. 5, pp. 631–653, 1995.
19. S. Heidenreich and P. U. Foscolo, "New concepts in biomass gasification," Prog. Energy Combust. Sci., vol. 46, pp. 72–95, 2015, doi: 10.1016/j.pecs.2014.06.002.
20. H. Beohar, B. Gupta, V. K. Sethi, and M. Pandey, "Parametric Study of Fixed Bed Biomass Gasifier : A review," Int. J. Therm. Technol., vol. 2, no. 1, pp. 134–140, 2012.

21. S. M. Santos, A. C. Assis, L. Gomes, C. Nobre, and P. Brito, "Waste Gasification Technologies: A Brief Overview," Waste, vol. 1, no. 1, pp. 140–165, 2022, doi: 10.3390/waste1010011.
22. M. La Villetta, M. Costa, and N. Massarotti, "Modelling approaches to biomass gasification: A review with emphasis on the stoichiometric method," Renew. Sustain. Energy Rev., vol. 74, no. November 2016, pp. 71–88, 2017, doi: 10.1016/j.rser.2017.02.027.
23. N. Couto, A. Rouboa, V. Silva, E. Monteiro, and K. Bouziane, "Influence of the biomass gasification processes on the final composition of syngas," Energy Procedia, vol. 36, pp. 596–606, 2013, doi: 10.1016/j.egypro.2013.07.068.
24. J. C. G. da Silva, J. L. F. Alves, G. D. Mumbach, S. L. F. Andersen, R. de F. P. M. Moreira, and H. J. Jose, "Hydrogen-rich syngas production from steam gasification of Brazilian agroindustrial wastes in fixed bed reactor: kinetics, energy, and gas composition," Biomass Convers. Biorefinery, 2023, doi: 10.1007/s13399-023-04585-z.
25. S. K. Sansaniwal, K. Pal, M. A. Rosen, and S. K. Tyagi, "Recent advances in the development of biomass gasification technology: A comprehensive review," Renew. Sustain. Energy Rev., vol. 72, no. January, pp. 363–384, 2017, doi: 10.1016/j.rser.2017.01.038.
26. E. Aristizábal-Alzate, "Aplicación del concepto de biorrefinería a la pulpa de café, mediante extracción fitoquímica y procesos termoquímicos, para la obtención de productos de alto valor agregado," Instituoto Tecnológico Metropolitano de Medellín, 2019.
27. J. Lin et al., "Enhanced low-temperature performance of CO2 methanation over mesoporous Ni/Al2O3-ZrO2 catalysts," Appl. Catal. B Environ., vol. 243, pp. 262–272, 2019, doi: 10.1016/j.apcatb.2018.10.059.
28. Grimalt-Alemany, I. V. Skiadas, and H. N. Gavala, "Syngas biomethanation: state-of-the-art review and perspectives," Biofuels, Bioprod. Biorefining, vol. 12, no. 1, pp. 139–158, 2018, doi: 10.1002/bbb.1826.
29. X. Jia, X. Zhang, N. Rui, X. Hu, and C. jun Liu, "Structural effect of Ni/ZrO2 catalyst on CO2 methanation with enhanced activity," Appl. Catal. B Environ., vol. 244, no. June 2018, pp. 159–169, 2019, doi: 10.1016/j.apcatb.2018.11.024.
30. H. Knözinger and K. Kochloefl, "Heterogeneous Catalysis and Solid Catalysts," Ullmann's Encycl. Ind. Chem., 2003, doi: 10.1002/14356007.a05_313.
31. H. S. Fogler, Elementos de ingeniería de las reacciones químicas. Pearson Educación, 2001.
32. O. Levenspiel, "Ingenieria de las reacciones quimicas," Journal of Chemical Information and Modeling, vol. 53, no. 9. pp. 277–293, 2002, doi: 10.1017/CBO9781107415324.004.